phys. stat. sol. (b) **141**, 303 (1987)

Subject classification: 78.55; 71.35; 71.55; S11.1

Physikalisches Institut IV der Universität Düsseldorf (a)[1])
and Department of Physics, University of New Mexico, Albuquerque (b)[2])

Sensitized Luminescence of Pure and Doped $NaNO_2$ Single Crystals

II. Time-Resolved Experiments and Preliminary Analysis[3])

By

H. PUFAHL (a), J. KÖHLER (a), TH. SCHMIDT (a), D. SCHMID (a), and V. M. KENKRE (b)

The fluorescence decay times of pure $NaNO_2$ and of $NaNO_2$ doped with KNO_2 are measured for varying temperature and dopant concentration. Both, time-resolved and steady measurements are carried out and are found to be in agreement with each other. Energy transfer rates are deduced from the measurements and an attempt is made to interpret them with the help of a generalization of the standard sensitized luminescence theory which includes detrapping effects. The result of this attempt is a strong indication that the rates for trapping and detrapping in $NaNO_2$ are *not* interrelated via detailed balance and the conclusion drawn is that a deeper theoretical investigation is necessary to analyze the experiment quantitatively. However, a rough estimate of the singlet exciton hopping rate can be made, and is found to be in agreement with the results of an interpretation of the lineshape asymmetry. For triplet excitons in $NaNO_2$, it is shown that it is natural to conclude that energy transfer is motion-limited and that the motion is one-dimensional, in agreement with expectations based on the crystal structure of $NaNO_2$.

Die Fluoreszenzabklingzeiten von reinem $NaNO_2$ und von $NaNO_2$, das mit KNO_2 dotiert ist, wird in Abhängigkeit von der Temperatur und der Dotierungskonzentration gemessen. Parallel dazu durchgeführte Messungen der stationären Spektren liefern Ergebnisse, die mit denen der zeitaufgelösten Experimente verträglich sind. Anhand der Meßergebnisse werden Energieübertragungsraten bestimmt. Der Versuch, die Daten mit Hilfe einer verallgemeinerten Theorie der sensibilisierten Lumineszenz, die thermische Wiederbefreiung der Exzitonen einschließt, zu interpretieren, liefert deutliche Anzeichen dafür, daß bei $NaNO_2$ Einfang und Wiederbefreiung nicht der gewohnten Beziehung für thermisches Gleichgewicht unterliegen. Es ist offensichtlich eine Erweiterung des theoretischen Konzepts notwendig. Eine grobe Abschätzung der Hüpfraten der Singulett-Exzitonen liefert Werte, die verträglich sind mit Überlegungen zur Form der Exzitonenlinien. Für Triplett-Exzitonen werden deutliche Hinweise darauf gefunden, daß die Energieübertragung bewegungsbegrenzt und im wesentlichen eindimensional ist.

1. Introduction

In a previous publication (Part I of this paper) [1] we presented a study of the steady-state fluorescence and phosphorescence of $NaNO_2$ single crystals. If these crystals are doped with K^+ impurities, one observes several series of impurity-induced lines both in the fluorescence and phosphorescence spectra which can be assigned to perturbed NO_2^- ions. The temperature dependence of these lines was studied in detail. At low

---

[1]) Universitätsstr. 1, D-4000 Düsseldorf, FRG.
[2]) Albuquerque, NM 87131, USA.
[3]) Part I see phys. stat. sol. (b) **140**, 605 (1987).

temperature the ratio of their intensities to those of the unperturbed lines is considerably higher than the relative dopant concentration (more than two orders of magnitude). This indicates that an efficient energy transfer takes place from the unperturbed host NO_2^- ions, which initially are excited preferentially, to the perturbed NO_2^- ions, which act as traps. This situation is reminescent of the well-known observations in organic molecular crystals [2, 3].

However, the traps in $NaNO_2$ are shallow enough to cause detrapping. This fact makes energy transfer in $NaNO_2$ more complicated than in the typically studied organic systems, viz. anthracene doped with tetracene, in which the trap depth is large enough to allow the neglect of detrapping. In this work we present experimental results which are obtained by studying the fluorescence decay time of the unperturbed NO_2^- ions following pulse excitation and the influence of K^+ impurities on the observed decay times. We also present a preliminary analysis of the data. It is hoped that in combination with steady-state results, such observations will eventually yield a reliable model for energy transfer in $NaNO_2$.

2. Experimental

The crystals were grown and cleaved into optical samples using the procedures described in Part I. The samples were mounted in a variable temperature cryostat (Konti Kryostat IT, Cryovac) which allowed access to temperatures between 2 and 300 K. They were excited at $\lambda = 337.1$ nm using a nitrogen laser (M 1000, Lambda Physik, pulse width 3 ns FWHM, maximum pulse energy 1 mJ). For standard lifetime measurements the laser beam was only weakly focused (spot size about 4 mm $\times$ $\times$ 10 mm) in order avoid effects of non-linear phenomena, viz. annihilation. Spectral resolution of the fluorescence light was achieved using a grating monochromator (HRP2, Jobin Yvon, focal length 0.6 m with a holographic grating of 1800 lines/mm). The signals were detected using a fast photomultiplier (31024, RCA) and a high speed oscilloscope (7104, Tektronix) in combination with a digitizing camera (150-10, Thomson CSF) and a microcomputer (Psi 80, Kontron). The overall response time of the detection scheme, as determined from the response to a picosecond light pulse from a modelocked dye laser, was about 1 ns. Since the observed decay times were not very long compared to the laser pulse width, the observed signals had to be deconvoluted. This was achieved using Laplace transform techniques. The resulting limits of error in the observed lifetimes were estimated to be ± 0.5 ns. Details for this procedure are described in [4].

In order to extract information about energy transfer, it is essential to know the trap concentration as accurately as possible. Since the quantity varies considerably with the crystals, it has to be measured in each particular sample at the spot which is illuminated by the laser light. The only quantity which is directly accessible to experiment is the concentration of the dopant ion K^+. We have measured the ratio of the total intensities of the most intense impurity-induced lines (A, F and G in Fig. 2 of [1]) to those of the corresponding lines of unperturbed NO_2^- ions in numerous representative samples. Following this, the K^+ concentration in these samples was determined using atomic absorption spectroscopy[4]). In Fig. 1 we have plotted the ratio of the total intensities of the impurity-induced lines (Φ_G) to those of the unperturbed lines (Φ_H) in the 0–2 region (Fig. 1 a) and the 0–7 region (Fig. 1 b) at 4.2 K as a function of the K^+ concentration determined on each sample. Up to a dopant concentration of about

[4]) We are very grateful to Dr. E. Vaeth of Firma Henkel KGaA, Düsseldorf, for carrying out the necessary procedures for this determination of the dopant concentration.

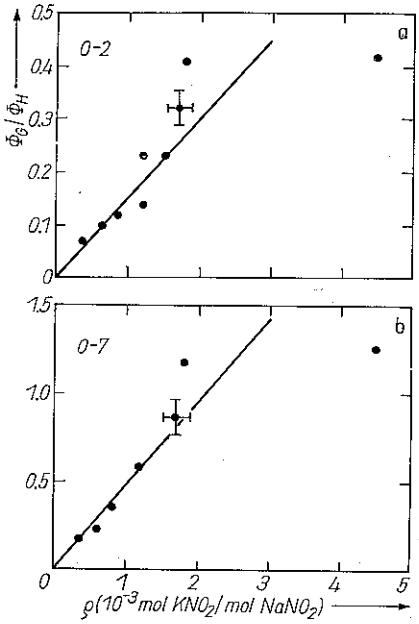

Fig. 1. Ratio of the intensities of the trap lines to those of the unperturbed host zero-phonon lines (Φ_G/Φ_H) in the a) 0–2 region and b) 0–7 region as a function of the dopant concentration (ϱ)

1.8×10^{-3} mol KNO_2/mol $NaNO_2$ the so-called quantum flux ratio Φ_G/Φ_H is proportional to the K^+ concentration ϱ with

$$\frac{\Phi_G}{\Phi_H} = 150\varrho \quad \text{for the 0–2 lines} \qquad (1)$$

and

$$\frac{\Phi_G}{\Phi_H} = 480\varrho \quad \text{for the 0–7 lines.} \qquad (2)$$

Using these relations, the K^+ concentration could be determined on each sample in situ. In undoped samples it was less than 20 ppm.

It was mentioned earlier that essential to the extraction of information about energy transfer from the experimental results is the accurate determination of the *trap* concentration. In order to estimate the number of traps resulting from one K^+ ion, we use Fig. 2 in which the projection of the orthorhombic unit cell into the *bc* plane is shown. If we assume that the body-centered $NaNO_2$ molecule is replaced by a KNO_2 molecule, we see that there are three inequivalent species of perturbed NO_2^- ions in the unit cell:

(i) the NO_2^- belonging to the impurity molecule in the center of the unit cell,

(ii) the NO_2^- ions on the left hand corners of the unit cell,

(ii) the NO_2^- ions on the right hand corners of the unit cell.

It seems reasonable to assign the three most intense progressions in the fluorescence spectra describe in [1] to these ions.

The intensity of all other trap lines was much weaker. Tentatively we may therefore assume that there are about nine relevant trap ions induced by each K^+ ion. However, the crystal structure of $NaNO_2$ suggests that excitonic energy transfer takes place preferentially along the *a* axis. (The length of the lattice constant *a* is only about 60% of that of *b* and *c*.) It will be shown in Section 4 that, at least in the case of triplet exci-

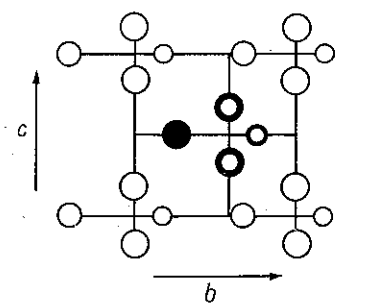

Fig. 2. Projection of the unit cell of $NaNO_2$ into the *bc* plane. The center molecule, which is above or below the plane of the corner molecules by an amount of $a/2$, is assumed to be the impurity. The most relevant trap states are probably the perturbed NO_2^- ions on the corners of the unit cell in addition to the NO_2^- belonging to the KNO_2 molecules

tons, this assumption is confirmed quantitatively by the experimental observations. Therefore it is reasonable to take the effective trap concentration ϱ_T to be approximately five times higher than the K^+ concentration ϱ. We use the factor five rather than nine because the two molecules which lie on the corners of the unit cell and whose projections into the *bc* plane coincide, act effectively as a single trap. These two molecules are not independent of each other and a linear exciton in the *a* direction can reach only one NO_2^- ion of each of them. Because of the uncertainty in this factor the experimental results in the following section are plotted as a function of the dopant concentration ϱ. For a quantitative interpretation, however, it should be kept in mind that ϱ_T is higher than ϱ.

3. Experimental Results

Fig. 3 a presents the fluorescence decay time of pure $NaNO_2$ single crystals as a function of temperature. The dots were obtained experimentally by observing the decay of the fluorescence on various zero-phonon lines following pulse excitation. The solid line was obtained by a least square fit to the experimental data. At 4.2 K the decay time is (8.3 ± 0.5) ns. When the temperature is increased, it decreases gradually to (7 ± ± 0.5) ns at 70 K and (6 ± 0.5) ns at 120 K. If one compares the behaviour to the temperature dependence of the quantum yield in the pure crystal (see Fig. 6 of [1]), one finds that the temperature dependence of the yield is considerably stronger than that of the lifetime. At 70 K, for instance, the quantum yield is only about 50% of its value at 4.2 K. The difference in the behaviour of the two quantities is probably due to the fact that the decay time measures the decay via all possible decay channels, whereas the quantum flux monitors only the decay via the radiative transition into intraionic vibrational states (with no interionic phonons participating). The temperature dependence of the Debye-Waller factors affects the two processes differently. We have not measured the temperature dependence of the total quantum yield, since the integration over the broad, weak phonon sidebands would result in uncertainties too large to yield significant results.

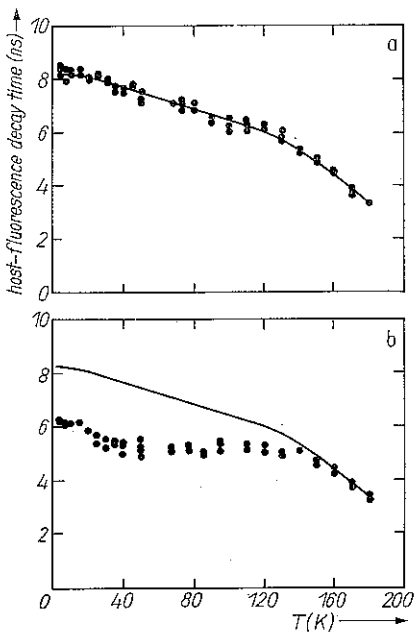

Fig. 3. Fluorescence decay times of a) pure $NaNO_2$ and b) $NaNO_2$ doped with 0.08% KNO_2 (●) as a function of temperature. The solid line shown in both parts of the figure presents a least square fit to the pure-crystal data

The part b of Fig. 3 illustrates the decrease of the fluorescence decay time caused by doping KNO_2 at a concentration of 0.08%. No deviation from an exponential decay was observed at any temperature or at any dopant concentration. Experience with similar experiments in organic molecular crystals suggests that we plot (see Fig. 4) the (dopant) concentration dependence of the difference between the in-

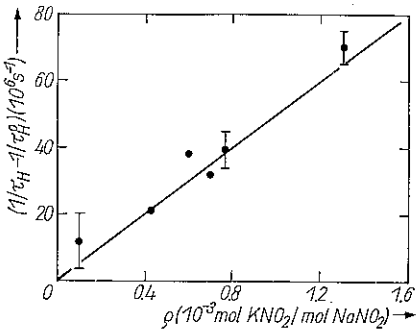

Fig. 4

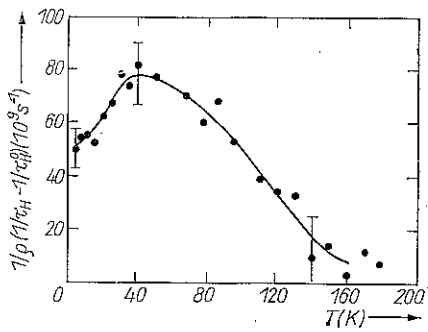

Fig. 5

Fig. 4. Energy transfer rate $k_{HG} = 1/\tau_H - 1/\tau_H^0$ as a function of dopant concentration ϱ at 4.2 K

Fig. 5. Normalized energy transfer rate $k_{HG}^+ = (1/\varrho)\, k_{HG}$ as a function of temperature. The solid line presents a least square fit to the data

verse fluorescence decay time observed on the zero-phonon lines of doped crystals $(1/\tau_H)$ and the corresponding quantity observed in pure crystals $(1/\tau_H^0)$.

Since this difference turns out to be proportional to the dopant concentration at all temperatures, we have normalized it by dividing the results obtained on various samples by the respective concentration before plotting, as in Fig. 5, its temperature dependence. In the case of organic molecular crystals like anthracene doped with tetracene, wherein thermal detrapping from excited guest states can be neglected, the quantity plotted in Fig. 5 is often called the normalized energy transfer rate (k_{HG}^0 or k'). We will use that terminology here and employ the superscript $+$ to indicate that the experimental quantity is normalized to the dopant concentration rather than the actual trap concentration.

If the intensity of the exciting laser pulse is increased by focusing the beam to a size of about 1×0.4 mm^2 on the surface of a pure crystal, one observes a distinct non-exponential decay of the fluorescence. This phenomenon is well known from molecular crystals and is ascribed to exciton–exciton annihilation. It is usually accounted for by the use of a phenomenonological nonlinear differential equation for the excited-state population of the host molecules:

$$\frac{dn_H}{dt} = I(t) - \frac{n_H}{\tau_H^0} - \gamma n_H^2 , \tag{3}$$

where $I(t)$ gives the rate at which excitons are created, γ is the annihilation constant and n_H is the density of excited host molecules. The annihilation constant γ can be determined from the solutions of (3) for homogeneous excitation and δ-shaped $I(t)$, provided the absolute value of $n_H(0)$ is known. Unfortunately in the experiments on $NaNO_2$ reported here, the excitation is not homogeneous as a result of Beer's law and of intensity variations across the laser beam's cross section, the pulse duration of the excitation is about 3 ns and thus not very short compared to the decay time and the absolute value of $n_H(0)$ can be estimated only very crudely. Only qualitative information about γ can be obtained. For this purpose, we fitted the observed decay curves with numerical solutions of (3), which were obtained by replacing the real exciton density $n_H(r, t)$ by a homogeneous average density, and estimated $n_H(0)$ from the pulse intensity and the excitation geometry. Values for γ obtained in this way are plotted in Fig. 6 as a function of temperature. Because of the crude approximation, the absolute

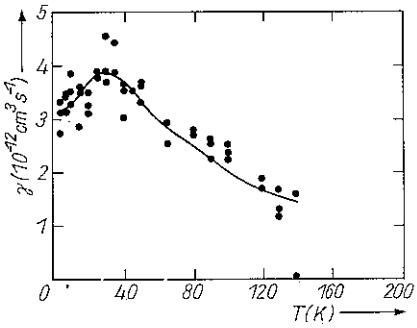

Fig. 6. Temperature dependence of the singlet-exciton annihilation constant. The solid line presents a least square fit to the data

value of γ should be considered only as an order of magnitude estimate. On the other hand the temperature dependence shown in Fig. 6 may be considered reliable.

4. Discussion

Most of the experimental results on sensitized luminescence in organic molecular crystals have been discussed in terms of a simple two-state model [2] for the excited state of the host and the guest (trap) molecules. In this model, the populations of these states are described by simple rate equations

$$\frac{\mathrm{d}n_\mathrm{H}}{\mathrm{d}t} = I(t) - \frac{n_\mathrm{H}}{\tau_\mathrm{H}^0} - k_\mathrm{HG} n_\mathrm{H}\,, \tag{4}$$

$$\frac{\mathrm{d}n_\mathrm{G}}{\mathrm{d}t} = k_\mathrm{HG} n_\mathrm{H} - \frac{n_\mathrm{G}}{\tau_\mathrm{G}^0}\,, \tag{5}$$

where k_HG is the energy transfer rate from the host to the guest, n_G denotes the density of excited guest molecules and τ_G^0 is the decay time of the excited guest molecules (radiative and nonradiative) in the absence of detrapping. The other quantities appearing in (4) and (5) have been defined earlier.

The energy transfer rate k_HG can be determined from (4) and (5) in two different ways:

(i) dynamically, i.e. from time-resolved experiments following pulsed excitation, and

(ii) statically, i.e. from quantum flux ratios in a steady state situation.

The latter method yields

$$k_\mathrm{HG/static} = \frac{1}{\tau_\mathrm{H}^0}\frac{\Phi_\mathrm{G}}{\Phi_\mathrm{H}}\,, \tag{6}$$

where Φ_G and Φ_H are the steady state quantum fluxes of guest and host fluorescence, respectively.

The time-resolved method results generally in

$$k_\mathrm{HG/dynamic} = -\frac{1}{n_\mathrm{G}}\left(\frac{\mathrm{d}n_\mathrm{H}}{\mathrm{d}t}\right) - \frac{1}{\tau_\mathrm{H}^0} \tag{7}$$

and, in the particular case of time-independent k_HG (equivalently, exponential $n_\mathrm{H}(t)$) encountered in most experiments, including the present ones on $NaNO_2$, in

$$k_\mathrm{HG/dynamic} = \frac{1}{\tau_\mathrm{H}} - \frac{1}{\tau_\mathrm{H}^0}\,, \tag{8}$$

where τ_H is the host-fluorescence decay time observed in the presence of energy transfer.

It might be useful to point out here that, whenever the deviation of the time dependence of n_H from that of an exponential is not discernible experimentally, $k_{HG/dynamic}$ is always equal to $k_{HG/static}$ as given by (6). This can be proved in a straight forward fashion by taking an appropriate Markoffian limit of the equations [5]. Being directly accessible to experiment, the right-hand-side expresssions in (6) and (8) can be plotted and compared. This is shown in Fig. 7. Except at the lowest temperature in the experiment, close agreement is seen between the static and dynamic expressions for k_{HG}. This implies that (i) $k_{HG}(t)$ is indeed independent of time for all practical purposes, and (ii) the quantum efficiencies of host and guest molecules are identical. The latter statement probably breaks down at the lowest temperatures because of the shallow traps. This can account for the difference between $k_{HG/dynamic}$ and $k_{HG/static}$ at those temperatures.

Contrary to the case of the typically studied organic molecular crystals (e. g. anthracene doped with tetracene), the simple two state model is not applicable to $NaNO_2$ for the following reasons:

(i) The trap depth in $NaNO_2$ is by no means large enough in relation to $k_B T$ to justify the neglect of thermal detrapping at higher temperatures.

(ii) Since only photons emitted in the zero phonon lines were recorded in the experiments, all the transitions which result in the phonon side bands act effictively as non-radiative transitions when the experimental results are to be discussed.

(iii) Energy transfer in $NaNO_2$, does not take place to a single type of traps, there being different traps with different trap depths and possibly different capture rates.

In order to account for the primary difference in $NaNO_2$ relative to molecular crystals, viz. non-negligible detrapping, a simple extension of (4) and (5) is necessary:

$$\dot{n}_H = I(t) - \frac{n_H}{\tau_H^0} - k_{HG} n_H + k_{GH} n_G \,, \tag{9}$$

$$\dot{n}_G = k_{HG} n_H - k_{GH} n_G - \frac{n_G}{\tau_G^0} \,, \tag{10}$$

where k_{GH} is energy transfer rate from the guest to the host caused by detrapping.

Since the two most important traps (F and G) which contribute almost 80% of Φ_G reveal a similar temperature dependence and have comparable trap depths (40 and 69 cm^{-1}, respectively), we will assume that there is only a single effective type of trap in $NaNO_2$ in the following discussion.

In the steady state, (9), (10) give

$$\left(\frac{1}{\tau_H^0}\right)\left(\frac{\Phi_G}{\Phi_H}\right) = \left[\left(\frac{1}{k_{HG}}\right) + \tau_G^0\left(\frac{k_{GH}}{k_{HG}}\right)\right]^{-1} \frac{\tau_G^0}{\tau_G^*}\,\frac{\tau_H^*}{\tau_H^0} \,. \tag{11}$$

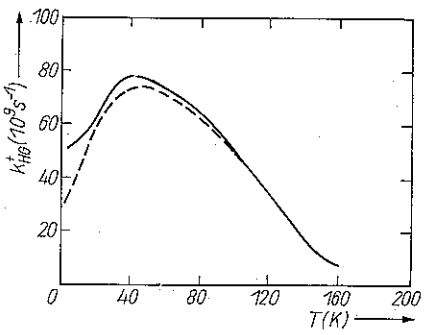

Fig. 7. Comparison of the results on the normalized energy transfer rate constants obtained from static spectra (– – –) and from time resolving experiments (———)

In (11), we have written the factors τ_H^*/τ_H^0 and τ_G^*/τ_G^0 explicitly to address the fact that the radiative lifetimes τ_H^* and τ_G^* are generally different from (longer than) the total lifetimes τ_H^0 and τ_G^0 of the host and guest, respectively.

Thus τ_H^0/τ_H^* and τ_G^0/τ_G^* are the radiative quantum efficiencies of the host and guest, respectively. The k's in (11) are static quantities. Equation (11) differs from (6) in that it contains the term $\tau_G^0(k_{GH}/k_{HG})$ which arises from nonnegligible detrapping. Under the simple assumption that the two k's are interrelated through detailed balance, the new term takes the form $(1/\varrho)\,\tau_G^0 \exp(-\beta\Delta)$ where $\beta = 1/k_B T$ and Δ is an appropriate energy difference. To ensure that the resulting formula has the support of a microscopic theory rather that of the phenomenological two-state model of equations (4), (5) or (9), (10), we give below the detailed formulation of the analysis of sensitized luminescence in the presence of detrapping. It involves a straightforward generalization of the usual theory [5, 6]. The outline of the generalization has been given earlier [5].

If $P_m(t)$ is the probability that the host site m is excited at time t, c is the rate at which excitation is trapped from the host molecule at site r (probability P_r) to the guest molecule (probability $P_{r\theta}$) with which it interacts, and c' is the rate of detrapping from the guest molecule to the host molecule at r, then

$$\frac{\mathrm{d}P_m}{\mathrm{d}t} + \frac{P_m}{\tau_H^0} = [\text{motion terms}] - \sum_r{}' \, \delta_{m,r}(cP_r - c'P_{r\theta}) \,, \tag{12}$$

where the prime over the summation sign signifies the inclusion of only the trap-influenced host sites in the summation. The motion terms may possess all the desired sophistication as required, including, if necessary, coherence in transport [6]. We do not display the specific form of those terms here because it is of no concern to the present discussion. If the trap concentration is low, we replace the summation [6] over traps by a single term in the standard way. One is thus led to

$$\frac{\mathrm{d}P_m}{\mathrm{d}t} + \frac{P_m}{\tau_H^0} = [\text{motion terms}] - \delta_{m,r}(cP_r - c'P_\theta) \,, \tag{13}$$

$$\frac{\mathrm{d}P_\theta}{\mathrm{d}t} + \frac{P_\theta}{\tau_G^0} = cP_r - c'P_\theta \,, \tag{14}$$

where we have replaced the index $r\theta$ by θ and have provided (14), the evolution for the guest probability P_θ. Equation (14) is solved formally with the help of Laplace transforms to give

$$\tilde{P}_\theta(\varepsilon) = \left(\varepsilon + \frac{1}{\tau_G^0} + c'\right)^{-1} [P_\theta(0) + c\tilde{P}_r(\varepsilon)] \,, \tag{15}$$

where tildes denote Laplace transforms, and ε is the Laplace variable. As our interest lies only in the initial condition wherein the guest is *not* excited, we put $P_\theta(0) = 0$. Equation (15), when substituted in (13) gives then a closed equation for P_r

$$\frac{\mathrm{d}P_m}{\mathrm{d}t} + \frac{P_m}{\tau_H^0} = [\text{motion terms}] - \delta_{m,r} \int_0^t \mathrm{d}t' \, C(t - t') \, P_r(t') \tag{16}$$

$$C(t) = c\delta(t) - c' \exp\left[-\left(\frac{1}{\tau_G^0} + c'\right)t\right]. \tag{17}$$

The resulting modifications in the expressions for the Laplace transform of the luminescence intensities is simply obtained by replacing c by $\tilde{C}(\varepsilon)$, i.e. by $c[\varepsilon + (1/\tau_G^0)] \times \times [\varepsilon + (1/\tau_G^0) + c']^{-1}$. This means that the quantum yield expressions for Φ_H and

Φ_G, which are obtained by integrating the intensities over all time, equivalently by putting $\varepsilon = 0$, undergo the modification consisting of the replacement of $(1/c)$ by $[(1/c) + (c'/c)\,\tau_G^0]$. Thus,

$$\Phi_H = \left[1 - \Phi_G \left(\frac{\tau_G^*}{\tau_G^0}\right)\right] \left(\frac{\tau_H^0}{\tau_H^*}\right) \tag{18}$$

$$\Phi_G = \left(\frac{\tau_G^0}{\tau_G^*}\right) \left[\frac{\varrho_T \tau_H^0}{\frac{1}{c} + \frac{1}{M} + \left(\frac{c'}{c}\right)\tau_G^0}\right]. \tag{19}$$

M is defined as $M = [\int_0^\infty \exp(-t/\tau_H^0)\,\psi_0(t)\,dt]^{-1}$, where $\psi_0(t)$ is the exciton self propagator, i.e. the probability that an exciton initially placed at a site is at that site at a later time t.

The simplest physical model of detrapping would require that the detrapping rate c' is related to the trapping rate c via detailed balance

$$\frac{c'}{c} = \exp(-\beta \Delta)\ , \tag{20}$$

where $\beta = 1/k_B T$ and Δ is the energy difference between the host excitation and the trap excitation. Under this assumption, (19) reduces to

$$\Phi_G = \left(\frac{\tau_G^0}{\tau_G^*}\right) \left[\frac{\varrho \tau_H^0}{\frac{1}{c} + \frac{1}{M} + \tau_G^0 \exp(-\beta \Delta)}\right]. \tag{21}$$

Equations (18) and (21) yield for the experimental observable

$$\frac{1}{\tau_H^0}\,\frac{\Phi_G}{\Phi_H} = \frac{\tau_G^0}{\tau_G^*}\,\frac{\tau_H^*}{\tau_H^0} \left[\frac{\varrho}{\frac{1}{c} + \frac{1}{M} + \tau_G^0 \exp(-\beta \Delta) - \varrho \tau_H^0}\right]. \tag{22}$$

Our efforts in applying (22) to the data on $NaNO_2$ have resulted in failure. In particular, it appears that the observations require a considerably larger trap depth Δ than spectroscopic evidence allows. Alternatively, it is necessary that the detrapping and the trapping rates (c' and c, respectively) are *not*-related via detailed balance. We have not been able to produce any simple rationale for such a modification of the model, although it appears that the data could be explained by a set of complicated assumptions regarding the relation of trapping and detrapping. A challenge therefore remains for the theorist: how to show, on natural grounds, that the detrapping rate in $NaNO_2$ should be at least an order of magnitude smaller than that given by detailed balance. We note here that the problem does not lie with the other details of the capture process we have used here. The same expressions would arise for almost any reasonable model of capture.

So far we have discussed only the case of singlet excitons. In the case of *triplet* excitons the situation is somewhat different. Again, there are two observables which depend on the exciton motion in a similar way namely the intensity of the sensitized phosphorescence in doped crystals and that of the delayed fluorescence in pure crystals which results from triplet–triplet annihilation. In Fig. 8 their temperature dependences are compared. Fig. 8a shows the total intensity of the trap phosphorescence zero-phonon lines (traps X and Z in Fig. 9 [1]) in arbitrary units. The maximum

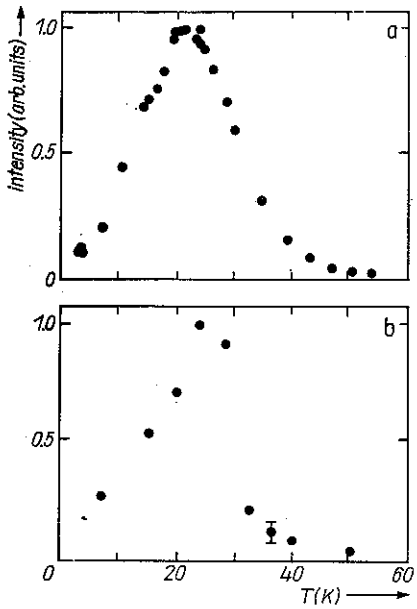

Fig. 8. a) Temperature dependence of the total intensity of the trap-induced phosphorescence lines (sensitized phosphorescence). Dopant concentration: 0.2% KNO_2. b) Temperature dependence of the total intensity of the delayed fluorescence in pure $NaNO_2$ [9]

trap-phosphorescence intensity is observed at about 24 K, it corresponds to a normalized quantum flux ratio of

$$\frac{1}{\varrho_T \tau_H^0} \frac{\Phi_G}{\Phi_H} = 3 \times 10^7 \text{ s}^{-1} .$$

At 4.2 K this quantity is about 4×10^6 s^{-1}. Using similar arguments as in the singlet case we have estimated the trap concentration ϱ_T to be about 3 times higher than the dopant concentration ϱ. We have taken this factor smaller than in the singlet case, because only two types of traps are seen in the phosphorescence spectrum. Fig. 8 b shows the temperature dependence of the intensity of the delayed fluorescence as given in [7]. As a result of the uncertainties in the initial exciton density, no absolute value of the annihilation constant could be given in this case, but the similarity between the two curves suggests that the limiting process in both cases is the triplet exciton motion, which influences both phenomena in an analogous way. It should be noted that the situation here is in sharp contrast to that for singlets in anthracene doped with tetracene or naphthalene doped with anthracene [8], where the trapping appears to be capture-limited.

There is an additional and independent piece of information which supports our suggestions that triplet trapping in $NaNO_2$ is motion-controlled. The average time a triplet exciton spends on an individual NO_2^- ion can be estimated from the motional narrowing of the electron spin resonance line (as compared to the hyperfine splitting observed on the traps) to be about 10^{-9} s at 4.2 K [9]. The hopping rate F, which is the reciprocal of this time, is therefore of the order of 10^9 s^{-1}. Kenkre [6] has shown that the motion rate M, which in the motion-limited case is identical to $(1/\varrho\tau_H^0)$ (Φ_G/Φ_H), is given by

$$M = \frac{(1 + 4F\tau_H^0)^{1/2}}{\tau_H^0} \tag{23}$$

for one-dimensional motion, by

$$M = \frac{4\pi F}{\ln (32 F \tau_H^0)} \tag{24}$$

for two-dimensional motion and by

$$M = 3.96F[1 + 0.32(F\tau_H^0)^{1/2}] \approx 4F \tag{25}$$

for three-dimensional motions. (The expressions (24) and (25) are approximations which hold in the limit of $F\tau_H \gg 1$, which certainly applies for the present problem. The corresponding exact expressions are given in [6]). With $\tau_H^0 \approx 10^{-4}$ s [10] we obtain from (23) to (25)

$$M = 6.3 \times 10^6 \text{ s}^{-1} \text{ for one-dimensional motion,}$$

$$M = 8.4 \times 10^8 \text{ s}^{-1} \text{ for two-dimensional motion, and}$$

$$M = 4 \times 10^9 \text{ s}^{-1} \text{ for three-dimensional motion.}$$

The calculated value of M for one-dimensional motion agrees quite well with the experimental value of $(1/\varrho\tau_H^0)\,(\Phi_G/\Phi_H)$, whereas the calculated numbers for two- or three-dimensional motion disagree with it by more than two orders of magnitude. This analysis supports the suggestion that sensitized phosphorescence in $NaNO_2$ is motion-limited and also justifies the assumption (made earlier by looking at the anisotropy of the crystal structure) that triplet exciton motion in $NaNO_2$ is one-dimensional.

We now return to the case of *singlet* excitons to discuss the unusual features observed in the lineshape studies presented in Part I [1]. There is a striking difference between the zero-phonon lines in the fluorescence spectrum of unperturbed $^{14}N^{16}O_2^-$ ions and those emitted by unperturbed NO_2^- with rare isotopic substituents or by traps. Whereas the latter are symmetrical, the former show a pronounced asymmetry with a characteristic shoulder on the low-energy side (see Fig. 12 of Part I).

We suggest that this difference arises from the breaking of the translational symmetry at the sites of isotopically substituted NO_2^- ions and of traps. The initial and the final state of unperturbed ions on a linear chain of translationally equivalent NO_2^- is best described in terms of Bloch functions resulting in an $E(k)$-dispersion relation. In the case of unperturbed NO_2^- the final states are (intramolecular) vibrationally excited states of the electronic ground state which are coupled via their dipolar interaction. One might thus explain the observed lineshape by postulating an $E(k)$ relation for the initial state (exciton) and the final state (vibron) as indicated qualitatively in Fig. 9. At low temperatures, according to this qualitative model, one expects to observe preferential emission from exciton states near $k = 0$. At higher

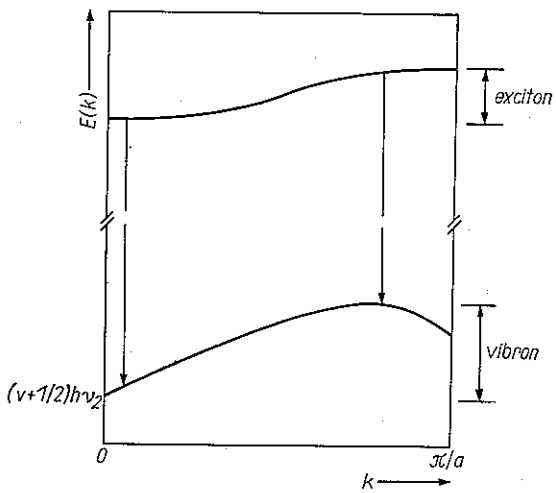

Fig. 9. Simplified band structure model for tentative explanation of the observed shapes of the singlet exciton fluorescence lines v and ν_2 are the vibrational quantum number and frequency of the bending mode of NO_2^- in the electronic ground state, respectively

temperatures all k-values participate according to the density of states in the initial and final state. In order to account for the temperature dependence of the lineshape, we can estimate the exciton bandwidth to be in the order of 5 to 10 cm^{-1} and the vibron bandwidth between 10 and 20 cm^{-1}.

It is satisfying to observe that the estimate of the exciton bandwidth obtained thus from the lineshape is in good agreement with a rough estimate that one may make from the energy transfer experiments for $T = 4.2$ K. In Section 3 we have estimated that the energy transfer rate per *impurity* (K^+) ion (see (2)) is

$$k^+_{HG} = \frac{1}{\varrho}\left[\frac{1}{\tau_H} - \frac{1}{\tau^0_H}\right] \approx 5 \times 10^{10}\ s^{-1} \quad \text{at } 4.2\ K\,.$$

The energy transfer rate per *trap* ion was estimated to be about 1/5 of this value

$$k^0_{HG} = \frac{1}{\varrho_T}\left[\frac{1}{\tau_H} - \frac{1}{\tau^0_H}\right] \approx 1 \times 10^{10}\ s^{-1}\,.$$

Although we do not have direct knowledge of the dimensionality of *singlet* exciton motion, similarity with the case of triplet excitons, discussed earlier in this section, as well as the crystal structure of $NaNO_2$ could prompt us to assume, tentatively, that singlet motion is also one-dimensional. A further assumption that singlet energy transfer is motion-limited leads to $k^0_{HG} \hat{\approx} M$. Using (23) we obtain the hopping rate $F = [(M\tau^0_H)^2 - 1]/4\tau^0_H \approx 2 \times 10^{11}$ Hz and therefore the interaction potential $V = hF/4 \approx 3.3 \times 10^{-23}$ J ≈ 1.7 cm^{-1}. The resulting exciton bandwidth is $\Delta E = 4\,V \approx 6.8$ cm^{-1} which is indeed in good agreement with the bandwidth estimated above from the lineshape.

Analogous model calculations for two- or three-dimensional motion yield estimates for the exciton bandwidth which are 2 to 3 orders too small to be compatible with the lineshape studies. Thus, this tentative analysis seems to support the mode of motion-limited, one-dimensional singlet-exciton energy transfer.

Although in the frame work of this model it is possible to explain the observed lineshapes qualitatively, it should be emphasized that the model is not able to account for additional details, for instance, for the additional substructure in the shoulders of the unperturbed zero-phonon lines (see Fig. 10 of Part I). It could for instance be due to singularities in the densities of states in the exciton and the vibron bands, but there is no information about such singularities. On the other hand, it could be due to out of plane librational motion of the NO_2^- ions. In this case, however, the absence of the structure on the lines from the isotopically substituted ions would be difficult to explain. At the present state of information, the model has to be considered as no more than preliminary.

Acknowledgements

Preliminary results concerning the static spectra of the sensitized fluorescence and the lineshape were already obtained by L. Schmidt at the Universität Stuttgart, Physikalisches Institut, Teil 3 [11]. Helpful discussion with Dr. L. O. Schwan are gratefully acknowledged. This work was supported by a grant from Sondermittel für Forschungsförderung des Ministers für Wissenschaft und Forschung des Landes Nordrhein-Westfalen, by the Deutsche Forschungsgemeinschaft under Grant number Schm 270/4-1 and by the National Science Foundation under Grant number 85-0638.

References

[1] F. Lisse, J. Köhler, H. Pufahl, and D. Schmid, phys. stat. sol. (b) **140**, 605 (1987).
[2] H. C. Wolf, Adv. atom. Mol. Physics **3**, 119 (1967).
[3] R. C. Powell and Z. G. Soos, J. Lum. **11**, 1 (1975).
[4] H. Pufahl, Dissertation, Universität Düsseldorf, 1986.
[5] V. M. Kenkre and Y. M. Wong, Phys. Rev. B **23**, 3748 (1981).
[6] V. M. Kenkre in: Exciton Dynamics in Molecular Crystals and Aggregates, Ed. G. Höhler, Springer-Verlag, Berlin 1982.
[7] L. Schmidt, H. Port, and D. Schmid, Chem. Phys. Letters **51**, 413 (1977).
[8] V. M. Kenkre and D. Schmid, Chem. Phys. Letters **94**, 603 (1983).
[9] W. Dietrich and D. Schmid, phys. stat. sol. (b) **74**, 609 (1976).
[10] W. Dietrich, F. Drissler, D. Schmid, and H. C. Wolf, Z. Naturf. **28a**, 284 (1973).
[11] L. Schmidt, Dissertation, Universität Stuttgart, 1978.

(Received November 11, 1986)

Note added in proof:

Recent experiments using absorption and fluorescence-excitation spectroscopy have shown that the assignment of ground state vibrational quantum numbers as given in Part I was erroneous for traps A, F and G. Consequently the trap depths quoted in Part I should be changed to (-1040 ± 1), (-858 ± 1) and (-885 ± 1) cm^{-1} for A, F and G, respectively. This reinterpretation resolves the apparent discrepancies in the interpretation of $k_{HG}(T)$. Details will be published in a subsequent paper.